Available online at www.ujpronline.com
Universal Journal of Pharmaceutical Research
An International Peer Reviewed Journal
ISSN: 2831-5235 (Print); 2456-8058 (Electronic)

RESEARCH ARTICLE

EXTRACTION AND CHARACTERIZATION OF PHARMACEUTICAL GRADE MICROCRYSTALLINE CELLULOSE FROM *RAPHIA FARINIFERA* INFLORESCENCE

Emmanuel Agboeze[1*], Uchechukwu Theresa O[2], Okoro Ogbobe[1]
[1]*Department of Industrial Chemistry, Enugu State University of Science and Technology, Nigeria.*
[2]*Department of Chemistry, Alex Ekwueme Federal University, Ndufu-Alike, Nigeria.*

Article Info:

Article History:
Received: 6 June 2022
Reviewed: 9 July 2022
Accepted: 23 August 2022
Published: 15 September 2022

Cite this article:
Agboeze E, Theresa OU, Ogbobe O. Extraction and characterization of pharmaceutical grade microcrystalline cellulose from *Raphia farinifera* inflorescence. Universal Journal of Pharmaceutical Research 2022; 7(4):59-67.
https://doi.org/10.22270/ujpr.v7i4.816

***Address for Correspondence:**
Emmanuel Agboeze, Department of Industrial Chemistry, Enugu State University of Science and Technology, Nigeria. Tel- +234 903 923 9802; E-mail: *emmanuel.agboeze@gmail.com*

Abstract

Background and objective: Microcrystalline cellulose (MCC) is a multifunctional polymer frequently used in the biomedical, food, and chemical industries. *Raphia Farinifera* Inflorescence (RFi), used to make palm wine in many parts of Africa, is frequently discarded as waste. The current study examines the extraction and characterization of pharmaceutical-grade MCC from RFi (RFi-MCC).
Method: Extraction was achieved by first defatting before sequentially treating RFi with alkali, dilute sulfuric acid (acid hydrolysis), and bleaching (H_2O_2).The RFi-MCC powder properties such as the True density, tapped density, bulk density, angle of repose and hydration capacity were observed.
Results: Microcrystalline cellulose showed distinctive peaks in the Fourier transform infrared spectroscopy (FT-IR). The scanning electron microscopy with Energy disperse spectroscopy (SEM/EDS) showed the variation in the elements, morphology of the fibers and the formation of RFi-MCC of approximately 100 µm. According to a thermogravimetric, BET and X-ray diffraction study, RFi-MCC degrades at 286°C, surface area of 1797.39 m^2/g and 336°, and exhibit crystallinity index of 0.67% respectively.
Conclusions: The findings show that the RFi fibers would be a valuable source of microcrystalline cellulose for utilization in the pharmaceutical, papermaking, and binder industries due to their powder characteristics, compressibility, and excellent swelling.
Keywords: biodegradable resources, biowaste utilization, microcrystalline cellulose, pharmaceutical grade cellulose, *Raphia Farinifera* Inflorescence.

INTRODUCTION

In order to meet the need for food crops, the current growth in the world's population has caused an increase in food production[1]. Agriculture residues are created in significant amounts around the world as a result of rising agricultural productivity. Yet cellulose, a major component that can be separated and employed in the creation of new biodegradable materials, is present in significant amounts of these wastes, which remain underutilized[2].Different plants contain cellulose from agricultural waste in varying amounts, such as cotton[3], grass[4], wood, banana peels, and rice husk[5].
Organic matter, which includes cellulose, lignin, hemicellulose, pectin, and other bound substances including water and extractives, makes up the walls of plants. Numerous researchers have reported multiple techniques that can isolate cellulose, but the soda process typically entails delignification with an alkali solution, followed by bleaching. These steps impact the cellulose crystal structure, aspect ratio, and morphology, and it has been reported that these effects depend on the particle extraction process, source materials, and methodology[6,7]. The fact that cellulose is biodegradable, fibrous in form, and comprises both crystalline and amorphous sections is a benefit. When lignin is subjected to an alkali treatment, it is transformed into black liquor, which aids in strengthening and fortifying the plant cell wall. It is made up of amorphous areas and various phenolic groups. Pentose and hexose sugars make up the branching polysaccharide known as hemicellulose[8,9]. Cellulose is the only abundant renewable biopolymer that has linear homopolysaccharides and a structure that alternates between an amorphous and crystalline region with repeating units of β-(1→4) connected D-glucose on Earth. Because of its accessibility and distinctive qualities, such as durability, non-toxicity,

and environmental biocompatibility, cellulose has recently attracted much study attention. Consequently, it is used in various applications, including food, pharmaceutical, cosmetic, and reinforcing polymer sectors industries[10,11,12].

Development of cellulose modification by mineral acids to degrade the bulk of the amorphous region and reduce the cellulose fiber to microns yielded commercial microcrystalline cellulose (MCC)[13]. Microcrystalline cellulose has been reported as purified, hydrolyzed and partly depolymerized cellulose prepared by treating α-cellulose pulp obtained from fibrous plant materials with excess mineral acid[14]. MCC is an intriguing cellulose derivative commercially made for the food and pharmaceutical industries. MCC is mainly used as a filler binder for indirect tablet compression since it is a diluent with high binding capabilities. It is an excellent dry binder at low concentrations. Other substances, especially active medicinal compounds that are difficult to tablet, can be effectively bound by MCC[15,16]. Recently several agricultural residuals have been employed in the preparation of pharmaceutical-grade MCC. However, these plant materials' chemical composition, choice of drying, solvents and structural organization may affect the composition of the α-cellulose extract and, subsequently, the crystallinity of the MCC produced[17]. Microcrystalline cellulose is considered the new environmentally friendly and sustainable option for adsorption of materials like persistent chemicals, dyes and metals. MCC isolated from RFi fiber can also be a filler material in the building industry, where it can enhance structural properties such as tensile strength, shear strength, and bearing capacity. However, chemical crosslinking and functionalization of the fibers could expand its applications. This would make RFi cellulose an intriguing possibility for the covalent immobilization of high molecular weight nitrogenous substances such as polypeptides like antibodies, gelatin, enzymes, collagen, and chitosan.

This research aimed to isolate and analyze pharmaceutical grade cellulose from waste residuals of *R. farinifera* inflorescence. The percentage structure, yield, and surface morphology of the fibers were investigated to determine the physical characteristics of the fibers. The several functional groups in the synthesized RFi-MCC powder were identified using FT-IR, TGA to determine the thermal energy of RFi-powder, SEM/EDS for morphology properties and chemical makeup RFi-MCC, respectively. Among other techniques, an XRD was utilized to determine the microstructure of RFi-MCC[18].

MATERIALS AND METHODS

Sample preparation

R. farinifera inflorescence (RFi) was collected at Mbu-Amon in Isi-Uzo Local Government Area, Enugu State, Nigeria and was identified in the Applied Biology Department, Enugu State University (ESUT), Enugu. RFi was washed with deionized water, sun-dried for two weeks, and chopped in a cutter to have the proper size material for pulverization. The sun-dried chopped RFi was pulverized and sieved to different particle sizes that range between 0.092 - 1.500 mm to increase the surface area and enhance further treatment. The Enugu State University research lab provided all the chemicals for pulping and bleaching.

Pretreatment of RFi waste

Dewaxing

The method employed by Agboeze *et al*., was used with a few modifications[19]. A total of 100 g of pulverized RFi was placed in the Soxhlet apparatus with boiling chips (7) in a flat-bottom flask. A mixture of toluene and ethanol in a ratio of 2:1 was added to the flask by measuring 250 ml of toluene and 125 ml of ethanol to remove chlorophyll pigments and waxes. The flask was subsequently placed on the heating mantle. The Soxhlet apparatus was assembled by attaching rubber hoses to the water outlet, condenser, and sink to supply cooling water to the system. The toluene ethanol mixture was heated to the boiling point before being adjusted to a steady boil eight times. The cooling water flow was adjusted frequently to provide high cooling conditions. After ~6 hours, the heating mantle was switched off and unplugged. Cooling water running was left for ~20 minutes until the apparatus had cooled down to minimize evaporation. After retrieving the boiling chips, the filtrate (toluene-ethanol mixture) was disposed of in the trash separately after drying. The residue (dewaxed RFi) was dried at room temperature, weighed afterward, and packed in a sealed plastic bag for further analysis.

Isolation of α- cellulose by pulping/delignification

The method employed by Agboeze *et al*.,[19] was adopted with modification. A total of 300 g of the dried dewaxed RFi was placed in a stainless-steel container to which 4.0 L of 3.5 percent w/v nitric acid and 0.1 percent sodium sulfite was added. For two hours, the mixture was allowed to digest. At 90 °C in a water bath (FGL 1083 Karl Kolb Scientific), remove lignin in soluble nitro-lignins, followed by thorough washing with water. It was treated with 4.0 L of 17.5 percent w/v sodium hydroxide at 80°C for one hour before discarded. The produced cellulose was properly cleaned with distilled water before being used.

Bleaching

After whitening with a 1:3 aqueous dilution of hydrogen peroxide for 60 minutes at 80 degrees Celsius and 1:1 for 24 hours, the extraction procedure was completed by washing with water until neutral. For the remaining samples, the procedure was repeated. The cellulose fiber material was filtered manually with a calico towel to create lumps, then dried in a hot air oven at 58°C for one hour.

Preparation of microcrystalline cellulose (RFi – MCC)

The method of Ohwoavworhua was used[20]. About 40 g of the resulting alpha Cellulose pulp was hydrolyzed in a pyrex beaker using 1.2 L 2.5 mol/dm^3 hydrochloric acid at 100ºC for 15 mins. The hot mixture was transferred into cold tap water and stirred vigorously using a spatula, and the mixture was left to stand overnight. The MCC obtained was washed thoroughly until neutral and dried at 50ºC for 60 mins followed by

further milling, and the portion passing through a 0.7 mm sieve was stored in an airtight container[21].

Characterization of RFi-MCC

The physicochemical parameters and powder qualities of MCC obtained from the RFi sample were analyzed using standard techniques, as described below:

Organoleptic characteristics analysis

The organoleptic characteristics (color, aroma, and taste qualities), identity, solubility, pH, and properties of modified and unmodified cellulose produced from an RFi sample were determined using British Pharmacopoeia 2004 requirements[22].

Identification

Garba, Lawan, Zhou, Zhang, Wang and Ohwoav-worhua, and Adelakun[23,24] developed a standard test method to determine cellulose, which was used in this study. A 2 g portion of the RFi-C sample was subjected to an iodinated zinc chloride solution for 15 minutes. The violet-blue coloration of the powder indicates that it is microcrystalline cellulose.

Solubility

Tests were carried out on the solubility of the sample in a variety of organic solvents, including water, dilute sodium hydroxide, alcohol, dilute HCl, and diethyl ether.

pH

RFi-C pH was determined by mixing 1 g of powder with 50 cm^3 distilled water for 5 minutes, and the pH of the supernatant was analyzed using a pH meter to obtain the final pH of the mixture.

Fourier-transform Infrared (FTIR) Spectroscopy analysis

To investigate the functional groups contained in the modified and unmodified RFi samples, a Fourier transform infrared spectrophotometer [Buck 530IR] from England was used. The transmittance approach was employed in this investigation. The Fourier-transform infrared spectrum of the RFi-C sample was captured on the KBr disc using a Fourier-transform technique. The sample was scanned between 4550 and 650 cm^{-1} at a resolution of 8 cm^{-1} with a scanning range of 4550 to 650 cm^{-1}.

X-ray Diffraction (XRD)

The XRD patterns were obtained using advanced equipment such as a Bruker D8 (X-ray diffractometer) with Cu K radiation, variable divergence and anti-scatter slits (illuminated length=10 mm), and a post-diffraction monochromator after the samples were dried. Data were taken from 10 to either 75 or 90 degrees Celsius, 2θ at intervals of 0.2 seconds at 25 degrees Celsius. Following the "Segal method"[25,26], the crystallinity index (CrI) was computed by dividing the height ratio between the intensity of the crystalline peak (I_{200}–I_{am}) and the total intensity (I_{200}) after subtracting the background signal. Topas (v4.2, Bruker AXS) was used to perform nonlinear least-squares fitting of the data, with the crystalline component estimated from the cellulose I structure given by the American Chemical Society[27,28]. For the crystalline and amorphous cellulose peaks, pseudo-Voigt line forms were utilized to represent them. For the backdrop and the degree of crystallinity obtained from the formula, a three-parameter 2nd order polynomial function was utilized.

$$CrI = \left(\frac{I_{200} - I_{am}}{I_{200}}\right) 100\%$$

$$l = \left(\frac{K\lambda}{\beta \cos\theta}\right)$$

Where K is the shape factor and Scherrer's constant = 0.89, I_{200} represent the greatest intensity of the (200) lattice diffraction peak at a 2θ angle between 22° and 23°, and I_{am} represents the minimum intensity of an amorphous area at a 2θ angle between 18° and 19°. The full width at half the height of the peak is denoted by β, while the radiation wavelength is denoted by λ[24,29].

Scanning electron microscopy equipped with Energy-dispersive X-ray spectroscopy (SEM/EDX)

A scanning electron microscope (Phenom Prox) from Phenom-World Eindhoven, the Netherlands, which was used to examine the surface morphology of modified and unmodified RFi cellulose powder. The microscope's resolution was 50 m (at a magnification of 1600x), and the depth resolution was approximately 0.5 mm. A high vacuum on the order of 102–103 Pa was used in conjunction with a high accelerating voltage of 15 kV to get measurements of the RFi. The dry method of preparation was utilized to pretreat the sample before usage.

Powder properties characterization

True density

The real density, Dt, of treated and untreated RFi-MCC powder was calculated using the liquid displacement method for both samples according to ASTM D standards. The immersion fluid used in this experiment was xylene, and the absolute density of the sample was calculated[30,31].

Bulk density

A total of 15 g of treated and untreated RFi-MCC powder was placed in a 100 cm3 measuring cylinder, and the sample's volume was recorded.

Tap density

The volume occupied by 15 g of RFi fiber after 50 taps on a laboratory bench with a height of 3.5 cm was measured.

Particle size distribution

In the range of 780 µm to 154 µm, test sieves were positioned in descending order. About 12.77 g of modified and unmodified RFi powder were deposited on the uppermost sieve, which was then shaken for 5 minutes in a JINLING Shaker (China) to quantify the weight of the powder retained on each sieve.

Powder flow properties

The Hausner index, Carr's index, angle of repose, and porosity of RFi-MCC powder are some of the properties that influence the flowability of modified RFi-MCC powders, respectively. These characteristics are discussed in greater detail below.

Hausner's ratio

The Hausner index is a powder characteristic that affects the amount of interparticle friction between particles. An increase in the Hausner index of more than 1.25 indicates good flow, while an increase in the Hausner index of less than 1.25 indicates poor flow[32]. The Hausner index could be calculated by dividing the

tap density by the bulk density, which was determined earlier.

Carr's index or degree of compressibility

Carr's index measures a powder's ability to shrink in volume over a given period[33]. It was possible to determine Carr's index percentage of RFi powders by using the values of bulk and tap densities previously obtained % Compressibility was calculated.

Loss of drying

A petri dish containing about 10 g of RFi-MCC sample powder was dried in a laboratory oven at a persistent temperature of 105°C until it reached a consistent weight. By dividing the mass of moisture by the weight of the sample and quantitatively expressing the result as a percentage, the percentage moisture loss may be calculated[24].

Moisture sorption capacity

In a tarred petri dish, 2 grams of RFi MCC sample powder was weighed and evenly placed over the surface of the container. The petri dish and its contents were put in a desiccator with distilled water in its reservoir (relative humidity RH=100 percent), kept at room temperature throughout the experiment. During the five-day experiment, we measured how much weight had been gained by the sample and determined how much water had been adsorbed based on that weight differential[35].

Hydration capacity

The Kornblum and Stoopak approach was employed in this investigation[36]. A 1 g quantity of the sample was deposited in four centrifuge tubes having a capacity of 15 mL, and the contents of each tube were made up of 10 mL of distilled water before being stoppered. The contents were shaken for two minutes using a JINLING Shaker (China). After that, the contents were left to rest for another 10 minutes to settle. The mixture was centrifuged at 1000 rpm for 10 minutes, after which the supernatant was carefully decanted, and the sediment was weighed. The hydration capacity of the residue was determined by dividing the weight of the silt by the weight of the dry sample.

RESULTS AND DISCUSSION

Multistage pulping was used to delignify the RFi waste. This method resulted in a homogenous α-cellulose pulp from the sample, and this shows that the pulping method was effective for the substantial removal of lignin. A total of 85.394% yield of α-cellulose pulp was obtained per 100 g RFi waste.

Physicochemical properties of RFi-MCC powder

The organoleptic properties of the RFi-MCC obtained were good as the material was granular, odorless, and white in colour. The RFi-MCC turned violet-blue on reacting with iodinated zinc chloride, identifying the powder as cellulose. The pH of the RFi-MCC was 6.15, which is within the official range of 5 -7.5[22]. The results of the physicochemical properties of RFi-MCC are shown in Table 1.

Powder properties characterization

Non-aggregated fibers can be spotted in RFI-MCC SEM micrographs. The dewaxing, pulping, and bleaching processes employed to remove wax, lignin, holo, and hemicellulose components may account for the smoother and non-spherical shape of the fibers exhibited in RFi-MCC. The SEM micrographs of the RFi-MCC and untreated RFi samples are shown in Figure 1 and Figure 2.

Table 1: Physicochemical properties of RFi-MCC.

Test	Result
Identification with iodinated zinc chloride	Turns violet-blue with iodinated $ZnCl_2$
pH	6.15
% NDF	33.4
% NDS	66.6
Ash insoluble in NDF	5.2
ADF	65.7
Ash insoluble in ADF	4.2
% Cellulose content	61.5
% Hemicellulose content	0.9
% Lignin content	33.4
%Moisture content	9.225
% Volatile matter	3.935
% Ash content	1.245
% Fixed carbon content	85.595
Iodine value	170.299
Density (g/cm^3)	0.565
Solubility Test	
Acetone: Water	Insoluble
Acetone	slightly soluble
Dil NaOH (5%)	Slightly soluble
Distilled water	Insoluble
Dil HCl (5%)	Insoluble
Ethanol	Insoluble
Methanol: Water	partially soluble
Diethyl ether	Insoluble

The EDS images for RFi-MCC and untreated RFi waste are shown in Figure 3 and Figure 4, with the component concentrations shown in weight percentages. The carbon, oxygen, Sulphur, and sodium peaks and their binding energies are depicted in Figure 4. It was mostly composed of carbon (64.5 wt percent) and oxygen (30 wt percent), with low amounts of minor impurities of Sulphur (3.8 wt percent) and sodium (1.7 wt percent). Bleaching and acid hydrolysis procedures, in which Na is present in the NaOCl acid employed in the bleaching process, are responsible for these increases in elemental contaminants. On the other hand, sulfur is found in H_2SO_4 acid, employed in acid hydrolysis, and on the untreated RFi. Even though dialysis was performed for several hours, Sulphur was detected considerably.

Table 2: Powder flow properties of RFI-MCC.

Parameter	Results
True density, g/mL	1.216
Bulk density, g/mL	0.429
Tap density, g/mL	0.577
Hausner's index	1.34
Carr's index%	25.75
Angle of repose	39.80°
Powder porosity %	64.7
Loss on drying %	5.89
Moisture sorption capacity %	46.81
Hydration capacity	2.80 (0.29)

Value in bracket represent standard deviation with n=3

The images were taken at a micrometer scale as it shows that it is 10 mm, and the distance between the lens and the sample was 8.4 mm. The surface seems composed of a not smooth surface due to hemi-cellulose, lignin, and other waxy components.

Table 3: The scale of flowability.

Carr's index	Hausner's index	Angle of repose	Flow character
10	1.00-1.11	25-30	Excellent
11-15	1.12-1.18	31-35	Good
16-20	1.19-1.25	36-40	Fair
21-25	1.26-1.34	41-45	Passable
26-31	1.35-1.45	46-55	Poor
32-37	1.46-1.59	56-65	Very poor
>38	>1.60	>66	Very very poor

It also reveals that the architecture is highly robust and tough. Figure 4 shows that the fibers were collected with a magnification of 8,000x. It was incredibly high magnification as the enlargement of the image size is 1,000 greater. The accelerating voltage is rather high, 20. KV, thus because the fibers are transformed into thin sheets of the polymer due to its different shapes and structure. The image is captured at 130 µm, and the distance between the lens and the picture is 8.4 mm. The image reveals that the surface is smooth because of eliminating lignin, hemicellulose, and waxy components.

Scanning electron microscope (SEM)

Figure 4 show that the fibers were collected with a 10,000 magnification, which means that the amplification of the RFi-MCC fiber appearance was bigger by 10,000. The accelerated voltage is 20.0KV which is pretty high. This is due to the sample's structural qualities and engineering (e.g., insulators, minerals). If the sample is a bit too rigid to tolerate a higher voltage, the voltage of the sample will be sufficient to raise the resolution yield, and it won't affect the blurriness of the image.

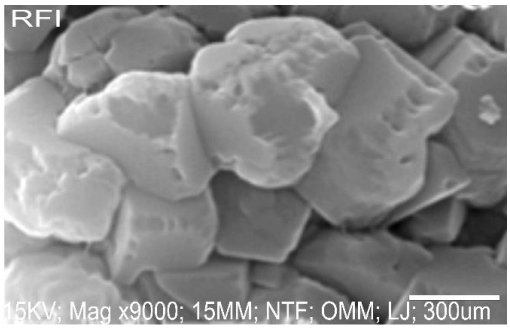

Figure 1: SEM micrographs of RFi-MCC.

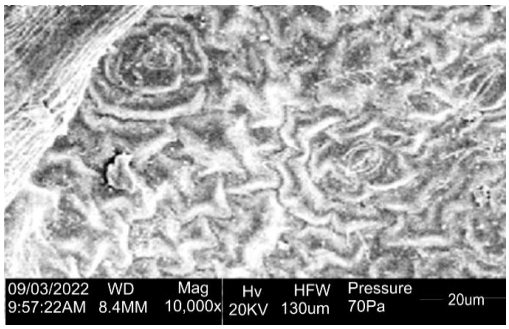

Figure 2: SEM micrographs of untreated RFi.

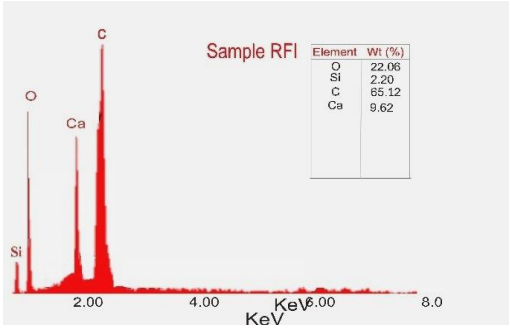

Figure 3: EDX analysis of RFi-MCC.

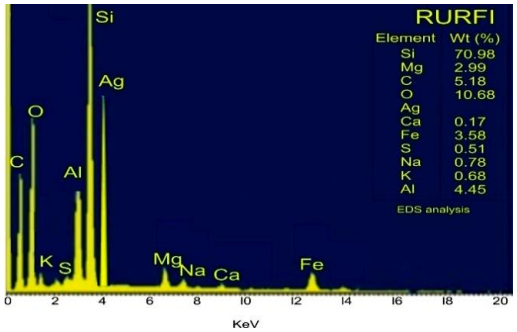

Figure 4: SEM micrographs of untreated RFi.

The FT-IR spectrum of RFi-MCC showed a characteristic spectrum of cellulose, according to[37]. Accordingly, the sample was presented in two main regions in the range of 600–1700 cm^{-1} and 2900–3500 cm^{-1}. The sample showed a wide band in the region between 2900 and 3500cm^{-1}, which specifies different intermolecular and intramolecular O-H stretching vibrations and OH groups present in the cellulose molecules. The spectra of the sample around 2901.990 cm^{-1} showed the characteristics of C–H stretching vibration. The vibration peak at 1420.1, 1312.0cm^{-1} is assigned to intermolecular C-H symmetric bending vibrations. The peak at 894.7cm^{-1} is due to the stretching vibration of the C-H and C-O-C groups. According to Huang, an increase in the intensity of this peak means a decrease in the crystallinity of the cellulose material. Pre-alkalization and alkalization steps reduce the hydrogen bonding vibration, reducing the hydroxyl groups by the reaction of NaOH.

X-ray diffractogram Analysis (XRD)

The XRD of the RFi-MCC, as shown in Figure 5, is characteristic of cellulose II with peaks appearing at about 12.50, 200, and 220 at 2θ (as a result of 101 and 002 reflections). The calculated crystallinity index is 0.66, which is within the range 0.58-0.69 reported by for 11 brand-names cellulose.

Particle Size distribution

The particle size of Rfi-MCC ranges from about 100-500 microns, with about 97% of the particle population less than 154 µm. It represents a unimodal frequency distribution that is negatively skewed.

Powder flow properties

Bulk density depends on the particles packing behavior which changes as the powder consolidates[41]. Higher

bulk density implies the need for larger amount for compressing tablet which is favourable in tableting due to reduction in the fill volume or so-called lower loading volume. The bulk density recorded 0.429, slightly above the USP specification of 0.32 (USP 32 – NF27), and the tapped density recorded 0.577. The flowability of MCC powder determines its suitability as a direct compression binder.

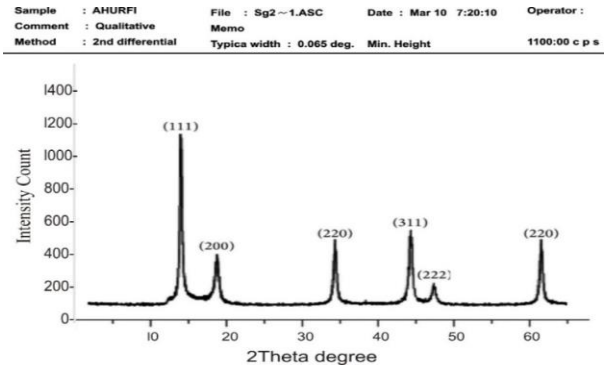

Figure 5: X–ray diffractogram of produced RFi-MCC.

Powder flowability is measured by the Hausner index, Carr's index, and angle of repose[42]. The higher the values of these parameters, the lower (poorer) the flow properties of the powder[43]. Table 2 shows the flow properties of the RFi– MCC powder. Hausner's index shows interparticle friction; a value greater than 1.25 shows poor flow[44]. Hausner's index for the RFI-MCC recorded 1.34.

Carr's index (compressibility index) shows the ability of a material to reduce in volume, and any value less than 16% indicates good flow while values above 35% show cohesion. RFI –MCC recorded a compressibility index of 25.75% while the angle of repose recorded 39.80ºC. The values of both Hausner's and Carr's indices and angle of repose shows that RFI – MCC flowed poorly according to the flowability scale in Table 3, but had better flow properties when compared with three MCCs obtained in literature examples GH – MCC (1.47, 31.72), [45]MCC – PP (1.379, 27.33)[46], CP – MCC (1.65, 39.5) [47] respectively. However, a glidant will be required to improve the flowability when using RFI–MCC in solid dosage forms formulations.

The loss on drying of RFI-MCC was 5.89% which is below the official limit of 6% (BP, 2004); this low value indicates the suitability of RFI-MCC as a diluent in the formulation of hydrolysable drugs.

Moisture sorption capacity measures a material's sensitivity to moisture, and this measurement is important because it shows the physical stability of tablets made with cellulose when stored under humid conditions. However, the moisture sorption capacity value for RFI-MCC was 10.8% which is low and is indicative that RFI-MCC has a high proportion of crystalline cellulose as the amount of water adsorbed by cellulose is proportional to the amount of amorphous cellulose present. This shows that tablets made from RFI-MCC will be stable. As a result, cellulose powders should be stored in any containers because of their non sensitivity to atmospheric moisture. The hydration capacity value of RFI-MCC is indicative that it's capable of absorbing less than two times its weight of water.

Thermogravimetric Results

The thermal stability of RFi fiber used as a filler or reinforcement in polymer composites is of paramount importance[48,49]. By mixing lignocellulosic materials with a polymer matrix at around 200 °C, you make composites that are strong and durable[48,49]. High temperatures during processing can cause lignocellulosic fiber degradation, which can result in undesired composite qualities such as odor and browning, as well as a reduction in mechanical capabilities[48,49]. The thermogravimetric curves for the RFi-MCC and natural RFi fibers studied are presented in Figure 6.

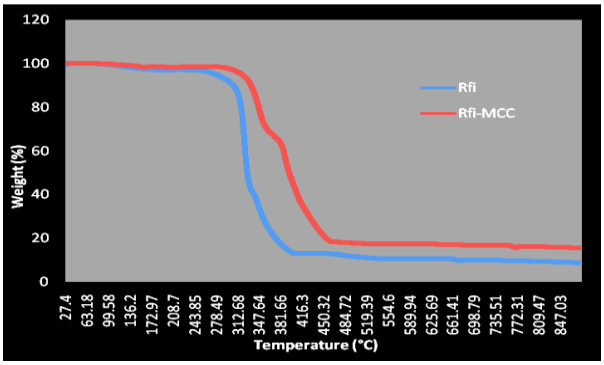

Figure 6: Thermogravimetric curve RFi-MCC and RFi.

All fibers studied lose water at roughly 100 °C, and subsequent thermal deterioration occurs in a three-step process. In the first phase, the breakdown of hemicellulose occurs at around 312.68°C for RFi-MCC and 340.53°C for RFi. After that, a second weight loss occurs at around 330.91°C and 360.81°C for RFi-MCC and RFi respectively, due to the main degradation of cellulose. Finally, the slow lignin degradation takes place between 84.364°C for RFi-MCC, 88.117°C for RFi and 490.67°C for RFi-MCC. According to Ramesh, hemicellulose depolymerization happens between 180 and 350°C, cellulose glycosidic linkage random cleavage occurs between 275 and 350 °C and 536.36°C, and lignin degradation occurs between 248 and 500°C[50]. Hemicellulose's increased thermal breakdown activity may be due to its chemical structure[48,50]. Hemicellulose is quickly hydrolyzed and has a haphazard amorphous structure. The cellulose molecule, on the other hand, is a lengthy polymer of repeated glucose units with crystalline sections that help lignocellulosic fibers maintain their thermal stability[48,49]. Lignin differs from hemicellulose and cellulose in that it is composed of three different types of benzene-propane units, is highly cross-linked, and has a very high molecular weight. As a result, lignin is highly thermally stable and difficult to decompose[48,50].

As can be seen in detail in Figure 6 above, at temperatures around 286–336°C, the RFi fibers showed a more significant weight loss. This tendency could be linked to the Rfi fiber's greatest extractive component, which is roughly 14%, as seen in Table 1. Extractives

have relatively low molecular mass than cellulose and, because of their increased volatility, can promote the RFi's ignitability at lower temperatures, speeding up the breakdown process. In this way, the degradation of one constituent may accelerate the degradation of the other RFi constituents. The major three components of RFi lignocellulosic fibers exhibit different thermal degradation properties depending on the proportion of cellulose, hemicellulose, wax, and lignin in each fiber. As a result, the chemical contents of fibers respond differently depending on whether they are isolated or densely mixed within each single cell of the fiber structure. The reduced lignin concentration and enhanced crystallinity of RFi could explain this phenomenon. As can be seen in Figure 6, RFi-MCC fibers have greater thermal stability than RFi-natural fibers. This could be due to the higher crystallinity index of the fibers, which is connected to lower levels of bound water and extractives.

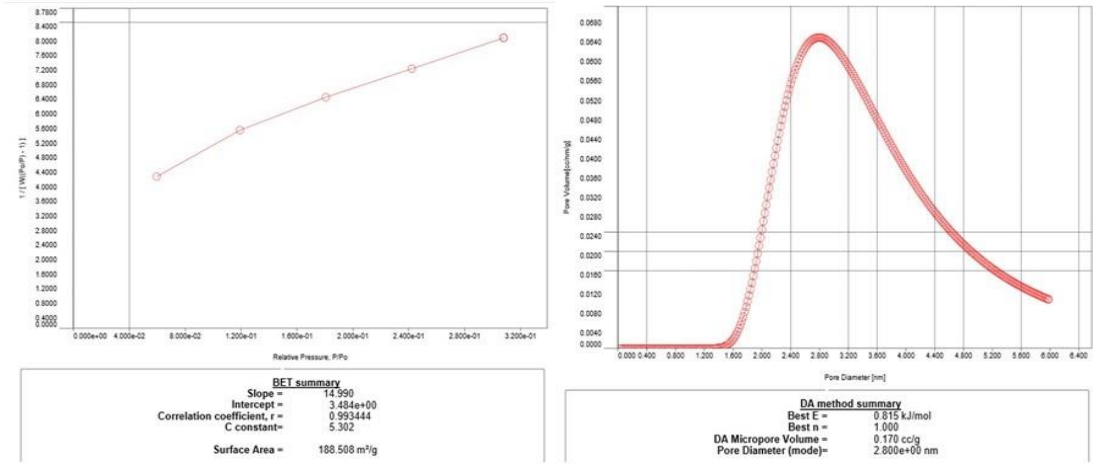

Figure 7: BET curve RFi-MCC and RFi.

BET analysis

Significant parameters like pore structure, porosity, adsorption site density, and specific surface area influence the physiochemical properties of the RFi. As a result, N_2 adsorption-desorption was employed to examine the pore volume, surface area, and diameter in both RFi-MCC. The N_2 adsorption/desorption isotherms of the RFi-MCC were shown in Figure 7. The RFi-MC had a step-shape isotherm of Type I, wherein a large amount of N_2 was adsorbed at low pressure (Quantity adsorbed =100 cm^3/g), indicating a strong interaction between N_2 molecules and the surface of the fiber[51]. All textural parameters related with RFi-MCC were show on the graph. The value of surface area for RFi and RFi-MCC samples were 188.508m^2/g, and 1797.39m^2/g, respectively. The surface area plays a very good role in the application of RF, high surface area means better adsorption[52]. Activation also led in an increment in the overall pore volume of the MCC. As a result, the addition of $ZnCl_2$ resulted in significant improvements in surface area and pore volume. This was in conformity with the results of a previous study[51,52].

Limitations of the study

This study is limited to extraction and characterization of microcrystalline cellulose from *R. Farinifera* inflourescence.

CONCLUSIONS

The value addition of agricultural waste is necessary for producing valuable products or raw materials for industrial use, which helps curb landfill menaces. *R. farinifera* inflorescence fibers are rich in cellulose and can thus be a good source of raw material for industrial applications. The extraction of MCC from *R. farinifera* inflorescence by defatting, alkali treatment, and bleaching processes was observed in the characterization analysis. Alkali treatment and bleaching with hydrogen peroxide reduced the fibers' sizes, increasing the final product's surface area. The swelling capacity of the isolated RFi-MCC could also be enhanced through modification of the surface hydroxyl groups by introducing groups such as carboxymethyl to form carboxymethyl cellulose. RFi-MCC powder obtained conformed well with USP specifications and British Pharmacopeial. RFi is a possible low-cost source of cellulose, microcrystalline, and reinforcing materials that can be used in the direct manufacturing of industrial products and other pharmaceutical applications.

ACKNOWLEDGEMENTS

The authors would like to appreciate staff members of Industrial Chemistry, University of Science and Technology, Enugu State, Nigeria, for their help during the study, interpretations and sample collection.

AUTHOR'S CONTRIBUTION

Agboeze E: writing original draft, conceptualization. **Theresa OU:** methodology, formal analysis, conceptualization. **Ogbobe O:** data curation, supervision. The final manuscript was read and approved by all authors.

DATA AVAILABILITY

The data and material are available from the corresponding author on reasonable request.

CONFLICT OF INTEREST

The authors affirm that there are no conflicts of interest.

REFERENCES

1. Correa S, Grosskopf AK, Lopez Hernandez H, *et al*. Translational applications of hydrogels. Chem Rev 2021; 121 (18):11385-11457. *http://doi.org/10.1021/acs.chemrev.0c01177*
2. Hanafi FNA, Kamaruding NA, Shaharuddin S. Influence of coconut residue dietary fiber on physicochemical, probiotic (*Lactobacillus plantarum* ATCC 8014) survivability and sensory attributes of probiotic ice cream. LWT 2022; 154:112725. *https://doi.org/10.1016/j.lwt.2021.112725*
3. Das R, Lindström T, Sharma PR, Chi K, Hsiao BS. Nanocellulose for sustainable water purification. Chem Rev 2022; 122(9): 8936–9031. *http://doi.org/10.1021/acs.chemrev.1c00683*
4. Seki Y, Selli F. Erdoğan ÜH, Atagür M, Seydibeyoğlu MÖ. A review on alternative raw materials for sustainable production: Novel plant fibers. Cellulose 2022; 29:4877–4918. *http://doi.org/10.1007/s10570-022-04597-4*
5. Aoudi B, Boluk Y, El-Din MG. Recent advances and future perspective on nanocellulose-based materials in diverse water treatment applications. Science Total Env 2022; 843:156903. *https://doi.org/10.1016/j.scitotenv.2022.156903*
6. Deepa B, Abraham E, Cordeiro N, *et al*. Utilization of various lignocellulosic biomass for the production of nanocellulose: A comparative study. Cellulose 2015; 22(2), 1075-1090. *http://doi.org/10.1007/s10570-015-0554-x*
7. Haldar D, Purkait MK. Micro and nanocrystalline cellulose derivatives of lignocellulosic biomass: A review on synthesis, applications and advancements. Carbohydrate Polymers 2020;250:116937. *https://doi.org/10.1016/j.carbpol.2020.116937*
8. Araújo T, Andrade M, Bernardo G, Mendes A. Stable cellulose-based carbon molecular sieve membranes with very high selectivities. J Memb Sci 2022; 641:119852. *https://doi.org/10.1016/j.memsci.2021.119852*
9. Krugly E, Pauliukaityte I, Ciuzas D, *et al*. Cellulose electrospinning from ionic liquids: The effects of ionic liquid removal on the fiber morphology. Carbohyd Polym 2022; 285:119260. *https://doi.org/10.1016/j.carbpol.2022.119260*
10. Shao X, Wang J, Liu Z, Hu, Liu NM, Xu Y. Preparation and characterization of porous microcrystalline cellulose from corncob. Indust Crops Produc 2020; 151:112457. *https://doi.org/10.1016/j.indcrop.2020.112457*
11. Sun B, Zhang M, Ni Y. Use of sulfated cellulose nanocrystals towards stability enhancement of gelatin-encapsulated tea polyphenols. Cellulose 2018; 25(9):5157-5173. *https://doi.org/10.1007/s10570-018-1918-9*
12. Abu-Thabit NY, Judeh AA, Hakeem AS, *et al*. Isolation and characterization of microcrystalline cellulose from date seeds (*Phoenix dactylifera* L.). Int J Biol Macro 2020; 155:730-739. *https://doi.org/10.1016/j.ijbiomac.2020.03.255*
13. BeMiller JN. One hundred years of commercial food carbohydrates in the United States. J Agricul Food Chem 2009; 57(18):8125-8129. *https://doi.org/10.1021/jf8039236*
14. Rowe R, Sheskey P, Quinn M. Handbook of Pharmaceutical Excipients, London: Pharmaceutical Press, 2009.
15. Chaerunisaa AY, Sriwidodo S, Abdassah M. Microcrystalline Cellulose as Pharmaceutical Excipient. In Pharmaceutical Formulation Design-Recent Practices. Intech Open 2019. *http://doi.org/10.5772/intechopen.88092*
16. Thoorens G, Krier F, Leclercq B, Carlin B, Evrard B. Microcrystalline cellulose, a direct compression binder in a quality by design environment—A review. Int J Pharm 2014; 473 (1-2): 64-72. *https://doi.org/10.1016/j.ijpharm.2014.06.055*
17. Thoorens G, Krier F, Rozet E, Carlin B, Evrard B. Understanding the impact of microcrystalline cellulose physicochemical properties on tabletability. Int J Pharm 2015; 490(1-2):47-54. *https://doi.org/10.1016/j.ijpharm.2015.05.026*
18. Caputo D, Fusco C, Nacci A, *et al*. A selective cellulose/hemicellulose green solvents extraction from buckwheat chaff. Carbohydrate Polymer Technologies and Applications 2021; 2:100094. *https://doi.org/10.1016/j.carpta.2021.100094*
19. Agboeze E. Modification of kola-nut testa cellulose for the removal of heavy metal in aqueous solution. Enugu State University of Science and Technology(ESUT), Enugu; 2018.
20. Ohwoavworhua FO, Kunle OO, Ofoefule SI. Extraction and characterization of microcrystalline cellulose derived from *Luffa cylindrica* plant. African J Pharm Res Dev 2004; 1(1): 1-6. *https://doi.org/10.1016/j.wasman.2018.10.023*
21. Singh AK, Singh A, Madhav NVS. Extraction and physicochemical characterization of novel potent mucoadhesive bio-material obtained from the fresh fruits pulp of *Achras zapotilla*. Universal J Pharm Res 2017; 2(6): 24-31. *http://doi.org/10.22270/ujpr.v2i6.R6*
22. Cartwright AC. The British Pharmacopoeia 1864 to 2014: medicines, International standards and the state, Routledge, 2016.
23. Garba ZN, Lawan I, Zhou W, *et al*. Microcrystalline cellulose (MCC) based materials as emerging adsorbents for the removal of dyes and heavy metals–A review. Sci Total Env 2020; 717:135070. *https://doi.org/10.1016/j.scitotenv.2019.135070*
24. Ohwoavworhua FO, Adelakun TA. Some physical characteristics of microcrystalline cellulose obtained from raw cotton of *Cochlospermum planchonii*. Tropical J Pharm Res 2005; 4(2):501-507. *http://doi.org/10.4314/tjpr.v4i2.14626*
25. Sidiras DK, Koullas DP, Vgenopoulos AG, Koukios EG. Cellulose crystallinity as affected by various technical processes. Cellulose Chemistry Technology 1990; 24:309–317.
26. Hassan ML, Berglund L, Abou Elseoud WS, Hassan EA, Oksman K. Effect of pectin extraction method on properties of cellulose nanofibers isolated from sugar beet pulp. Cellulose 2021; 28(1)7:10905-10920.
27. French AD. Idealized powder diffraction patterns for cellulose polymorphs. Cellulose 2014; 21(2):885-896. *https://doi.org/10.1107/S0021889886089458*
28. Schutyser W, Renders AT, Van den Bosch S, *et al*. Chemicals from lignin: An interplay of lignocellulose fract-ionation, depolymerisation, and upgrading. Chem Soc Rev 2018; 47(3):852-908. *http://doi.org/10.1039/C7CS00566K*
29. Seki Y, Kılınç AÇ, Dalmis R, Atagür M, Köktaş SGAA, Önay AB. Surface modification of new cellulose fiber extracted from *Conium maculatum* plant: A comparative study. Cellulose 2018; 25(6):3267-3280.
30. Maache M, Bezazi A, Amroune S, Scarpa F, Dufresne A. Characterization of a novel natural cellulosic fiber from *Juncus effusus* L. Carbohydrate Polym 2017;171:163-172. *https://doi.org/10.1016/j.carbpol.2017.04.096*
31. Siva R, Valarmathi TN, Palani Kumar T, Samrot AV. Study on a Novel natural cellulosic fiber from *Kigelia africana* fruit: Characterization and analysis. Carbohydrate Polym 2020; 244:116494. *https://doi.org/10.1016/j.carbpol.2020.116494*
32. Lau E. Preformulation studies. SS Satinder Ahuja, Ed., Academic Press 2001;173-224.
33. Qiu Y, Chen Y, Zhang GG, Yu L, Mantri RV. Developing solid oral dosage forms: pharmaceutical theory and practice, Second Edition ed., Academic press, 2017.

34. Adelakun TA, Ohwoavworhua FO. Some physical characteristics of microcrystalline cellulose obtained from raw cotton of *Cochlospermum planchonii*. Tropical J Pharm Res 2005; 4(2): 501-507. *http://doi.org/10.4314/tjpr.v4i2.14626*
35. Audu-Peter JD, Ojile JE, Bhatia PG. Physicochemical and powder properties of alpha-and microcrystalline-cellulose derived from maize cobs. J Pharm Biores 2004; 1(1):41-45.
36. Kornblum SS, Stoopak SB. A new tablet disintegrating agent: Cross-linked polyvinylpyrrolidone. J Pharm Sci 1973; 62(1):43-49: 1973. *https://doi.org/10.1002/jps.2600620107*
37. Huang C, Yu H, Abdalkarim SYH, *et al*. A comprehensive investigation on cellulose nanocrystals with different crystal structures from cotton via an efficient route. Carbohydrate Polym 2022; 279:118766. *https://doi.org/10.1016/j.carbpol.2021.118766*
38. Wang S, Wang Q, Kai Y. Cellulose nanocrystals obtained from microcrystalline cellulose by p-toluene sulfonic acid hydrolysis, NaOH and ethylenediamine treatment. Cellulose 2022; 1-10.
39. Agboeze E, Ogbobe O. J Innov Applied Res 2022; 5:1-12, 2022.
40. Ngounou EMD, Mang YD, Dongmo F, Malla OWI, Dongmo SS, Yanou NN. Effect of the aqueous extract of *Clerodendrum thomsoniae* Linn (verbenaceae) leaves on type 2 diabetic wistar rats induced by the MACAPOS1type diet and dexamethasone. Universal J Pharm Res 2021; 6(3):9-16.*https://doi.org/10.22270/ujpr.v6i3.601*
41. Nsor-Atindana J, Chen M, Goff HD, *et al*. Functionality and nutritional aspects of microcrystalline cellulose in food. Carbohydrate Polym 2017; 172:159-174.
42. Krassig HA. Cellulose: Structure, accessibility, and reactivity, Yverdon: Gordon and Breach Science 1993. *https://doi.org/10.1002/pi.1995.210360114*
43. Rowe RC, Sheskey P, Quinn M., Handbook of Pharmaceutical Excipients, Libros Digitales-Pharmaceutical Press 2009.
44. Haafiz MM, Eichhorn SJ, Hassan A, Jawaid M. Isolation and characterization of microcrystalline cellulose from oil palm biomass residue. Carbohydrate Polym 2013; 628-634. *https://doi.org/10.1016/j.ijbiomac.2017.05.135*
45. Ohwoavworhua FO, Adelakun TA, Okhamafe AO. Processing pharmaceutical grade microcrystalline cellulose from groundnut husk: Extraction methods and characterization. Int J Green Pharm 2009; 3(2):1-9.
46. Nwajiobi CC, Otaigbe JOE, Oriji O. Physicochemical, spectroscopic and tableting properties of microcrystalline cellulose obtained from the African breadfruit seed hulls. African J Biotech 2019;18:371-382.
47. Ohwoavworhua FO, Adelakun TA. Some physical characteristics of microcrystalline cellulose obtained from raw cotton of *Cochlospermum planchonii*. Tropical J Pharm Res 2005; 4(2):501-507. *http://doi.org/10.4314/tjpr.v4i2.14626*
48. Hasan KM, Horváth PG, Alpár T. Potential natural fiber polymeric nanobiocomposites: A review. Polymers 2020; 12, (5): 1072.
49. Mahmud S, KHasan KM, Jahid M, Mohiuddin K, Zhang R, Zhu J. Comprehensive review on plant fiber-reinforced polymeric biocomposites. J Mat Sci 2021; 56(1)2:7231-7264. *https://doi.org/10.1007/s10853-019-03990-y*
50. Ramesh M. Kenaf (*Hibiscus cannabinus* L.) fibre based bio-materials: A review on processing and properties. Progress Mat Sci 2016; 78:1-92.
51. Santmarti A, Zhang H, Lappalainen T, Lee KY. Cellulose nanocomposites reinforced with bacterial cellulose sheets prepared from pristine and disintegrated pellicle. Composites Part A:, Applied Science and Manufacturing 2020; 130, 105766. *https://doi.org/10.1016/j.compositesa.2020.105766*
52. Kondor A, Santmarti A, Mautner A, Williams D, *et al*. On the BET surface area of nanocellulose determined using volumetric, gravimetric and chromatographic adsorption methods. Front Chem Eng 2021; 3:738995. *https://doi.org/10.3389/fceng.2021.738995*